Biochemical and Biophysical Research Communications 493 (2017) 618–624

Contents lists available at ScienceDirect

Biochemical and Biophysical Research Communications

journal homepage: www.elsevier.com/locate/ybbrc

RAI3 knockdown promotes adipogenic differentiation of human adipose-derived stem cells by decreasing β-catenin levels

Chanyuan Jin [a, 1], Wensi Wang [a, 1], Yunsong Liu [a], Yongsheng Zhou [a, b, *]

[a] Department of Prosthodontics, Peking University School and Hospital of Stomatology, Beijing 100081, China
[b] National Engineering Lab for Digital and Material Technology of Stomatology, Peking University School and Hospital of Stomatology, Beijing 100081, China

ARTICLE INFO

Article history:
Received 23 August 2017
Accepted 24 August 2017
Available online 1 September 2017

Keywords:
RAI3
Adipogenic differentiation
Human adipose-derived stem cells
β-catenin

ABSTRACT

Retinoic acid-induced protein 3 (*RAI3*) has been found to play significant roles in embryonic development, cellular proliferation and differentiation, but its role in adipogenesis has not been explored. In this study, we discovered *RAI3* was downregulated during the adipogenic differentiation of human adipose derived stem cells (hASCs). Moreover, we demonstrated that knockdown of *RAI3* promoted adipogenic differentiation of hASCs both *in vitro* and *in vivo*. Mechanistically, our findings showed that inhibition of *RAI3* in hASCs reduced the expression of β-catenin, and lithium chloride which can activate the β-catenin pathway abolished the effect of *RAI3* knockdown on the adipogenesis. These results suggest *RAI3* plays an important role in adipogenesis of hASCs and may have a potential use in the future application.

1. Introduction

Adipose tissue plays key roles in storing energy, producing heat and acting as an endocrine organ to regulate various physiological and metabolic processes [1]. However, breast tumor resection, severe burns or injury can lead to adipose tissue defects. Thus, understanding adipogenesis will provide therapeutic strategies to replace the lost adipose tissue [2]. Adipogenic differentiation which is critical for adipose development refers to the process from preadipocytes into adipocytes and is regulated by complicated transcription factors and signaling pathways [3]. However, the exact underlying mechanism of adipogenic differentiation has not been fully elucidated and should be further investigated. Since adipose-derived stem cells (ASCs) can be easily harvested from adipose tissue and have a prominent ability to differentiate into mature adipocytes [4], we choose ASCs as a cell model for studying adipogenesis.

Retinoic acid-induced protein 3 (*RAI3*) is a member of the type 3-G protein-coupling receptor family and plays important roles in multiple cellular events. Its dysregulation may result in several different types of cancers and other diseases [5–8]. However, the roles of *RAI3* in adipogenesis are still unexplored.

Wnt/β-catenin pathway plays important roles in the differentiation of stem cells and β-catenin has been shown to inhibit adipogenesis [9]. β-catenin can be phosphorylated by GSK3β and degraded subsequently, while lithium chloride (LiCl) can activate Wnt/β-catenin signaling by blocking GSK3β-mediated phosphorylation of β-catenin [10].

In this study, we found that *RAI3* was downregulated in adipogenic differentiation of human adipose derived stem cells (hASCs). Knockdown of *RAI3* promoted adipogenesis of hASCs *in vitro* and *in vivo*. Finally, we demonstrated that *RAI3* knockdown promoted adipogenic differentiation of hASCs possibly via inhibiting β-catenin expression. These results reveal new insights into the mechanisms of adipogenic differentiation and provide a potential molecular target for adipose tissue engineering.

2. Methods

2.1. Cell culture

Primary hASCs from three donors were purchased from ScienCell Research Laboratories (Carlsbad, CA, USA) and cultured in standard growth media consisting of Dulbecco's Modified Eagle Medium (DMEM) with 10% fetal bovine serum and 1% antibiotics. For adipogenic induction, cells were cultured in standard growth media supplemented with 50 nM insulin (Sigma-Aldrich, St Louis, MO, USA), 100 nM dexamethasone (Sigma-Aldrich), 0.5 mM 3-

* Corresponding author. Department of Prosthodontics, Peking University School and Hospital of Stomatology, 22 Zhongguancun South Avenue, Haidian District, Beijing 100081, China.
E-mail address: kqzhouysh@hsc.pku.edu.cn (Y. Zhou).
[1] These authors contributed equally to this work.

http://dx.doi.org/10.1016/j.bbrc.2017.08.142
0006-291X/

isobutyl-1-methylxanthine (Sigma-Aldrich), and 200 μM indomethacin (Sigma-Aldrich). The medium was changed every 2 days. All cell-based *in vitro* experiments were repeated in triplicate.

2.2. Lentivirus infection

Viral packaging and infection was prepared as described previously [11]. Transfection of the hASCs was performed by exposing them to dilutions of the viral supernatant in the presence of polybrene (5 μg/mL) for 24 h. 72 h post transfection, puromycin (10 μg/mL) was added to select the stably transfected cells. The shRNA target sequences were as follows:

Non-targeting control shRNA (NC): TTCTCCGAACGTGTCACGTTTC.
sh*RAI3*-1: GCCTAGTCCAGGATGTTATCG.
sh*RAI3*-2: GTCGCAATGAAGACTTTGTCC.

2.3. Oil red O staining

At day 21, cells were washed with PBS, fixed with 10% formalin for 30 min and rinsed with 60% isopropyl alcohol. Oil red O (0.3%, Sigma-Aldrich) was then added and incubated for 10 min at room temperature. The stained cells were washed three times with distilled water, observed and imaged under a microscope. For quantitative assessment, stained cells were eluted with 100% isopropyl alcohol and quantified by spectrophotometric absorbance at 520 nm against a blank (100% isopropyl alcohol).

2.4. RNA isolation and qRT-PCR

Total RNA was extracted from cells with TRIzol reagent (Invitrogen, Carlsbad, CA, USA) according to the manufacturer's instructions. The cDNA was synthesized using the PrimeScript RT Reagent Kit (Takara, Tokyo, Japan). qRT-PCR was conducted with SYBR Green Master Mix (Roche Applied Science, Mannheim, Germany) on an ABI Prism 7500 real-time PCR System (Applied Biosystems, Foster City, CA, USA). The primers used for *RAI3*, proliferator activated receptor γ (*PPARγ*), CCAAT/enhancer-binding protein α (*C/EBPα*), *ADIPOQ*, and glyceraldehyde 3-phosphatedehydrogenase (*GAPDH*, internal control for mRNAs) are listed in Table 1.

2.5. Western blot analysis

Cells were collected, washed with PBS, and lysed in RIPA buffer. Proteins were measured and analyzed with a BCA protein assay kit (Thermo Scientific, Waltham, MA, USA). Equal amounts of protein from each sample were separated by 10% sodium dodecyl sulfate–polyacrylamide gel electrophoresis and transferred to a polyvinylidene fluoride membrane (Millipore, Billerica, MA, USA). After blocking, the membrane was incubated with primary antibodies specific against RAI3 (Cell Signaling Technology, Beverly, MA, USA), PPARγ (Cell Signaling Technology), β-catenin (HuaxingBio Science, Beijing, China), or GAPDH (Abcam, Cambridge, UK) at 4 °C overnight. The membranes were washed and subsequently incubated with secondary antibodies (Zhongshan Goldenbridge, Beijing, China) at room temperature for 1 h and then washed three times. Detection of each protein was conducted with the ECL Western Blot Kit (CWBIO, Beijing, China). The intensities of bands were quantified using ImageJ analysis software (http://rsb.info.nih.gov/ij/). GAPDH was used as an endogenous control and for normalization.

2.6. In vivo adipose tissue formation assay

All animal experiments were approved by the Peking University Animal Care and Use Committee. Cells were induced in the adipogenic differentiation medium for 1 week and then collected and incubated with Collagen Sponge (8 mm × 8 mm × 2 mm) for 2 h at 37 °C. The mice were housed with specific pathogen-free conditions and randomized into 3 groups of 10 mice each: NC group (implanted with adipogenesis-induced hASCs/Collagen sponge), sh*RAI3*-1, sh*RAI3*-2 group (implanted with adipogenesis-induced sh*RAI3*-hASCs/Collagen sponge). The complex was implanted subcutaneously into the back of the nude mice, retrieved at 8 weeks after implantation and prepared for histological observation.

2.7. Histological observation

The harvested implants were fixed with 4% paraformaldehyde and cut in half. One half was dehydrated, embedded with paraffin, and sectioned (5-μm-thick) for hematoxylin and eosin (H&E) staining, while the other half was embedded in a Tissue-Tek OCT freezing medium (Sakura Finetek Inc., Torrance, CA, USA) and cut into 7-μm-thick sections for Oil red O staining.

2.8. Statistical analysis

Analysis was performed using Prism (GraphPad Software, San Diego, CA, USA). All values are expressed as mean ± standard deviation (SD). Differences between two groups were analyzed by Student's *t*-test. In cases of two or more groups, one-way analysis of variance was performed. A *P*-value <0.05 was considered statistically significant.

3. Results

3.1. RAI3 is downregulated during adipogenic differentiation of hASCs

To determine whether *RAI3* is involved in adipogenic differentiation of hASCs, we first examined its expression during this process at different time points (0, 3, 7, 10 and 14 days). qRT-PCR showed the mRNA expression of *RAI3* decreased during adipogenesis of hASCs (Fig. 1A), while adipocyte marker genes such as peroxisome proliferator activated receptor γ (*PPARγ*), CCAAT/enhancer-binding protein α (*C/EBPα*), and *ADIPOQ* increased during this process (Fig. 1B–D). Consistently, western blot analysis revealed the protein expression of the adipogenesis key marker

Table 1
Primers used in qRT-PCR.

Name	Forward primer(5′→3′)	Reverse primer(5′→3′)
GAPDH	ATGGGGAAGGTGAAGGTCG	GGGGTCATTGATGGCAACAATA
RAI3	TGCTCACAAAGCAACGAAAC	TGGTTCTGCAGCTGAAAATG
PPARγ	GAGGAGCCTAAGGTAAGGAG	GTCATTTCGTTAAAGGCTGA
C/EBPα	CGCAAGAGCCGAGATAAAGC	CACGGCTCAGCTGTTCCA
ADIPOQ	CTTGCAAGAACCGGCTCAGATCCTCCC	GAGCTGTTCTACTGCTATTAGCTCTGC

PPARγ was upregulated during adipogenic differentiation of hASCs, while RAI3 was downregulated (Fig. 1E and F).

3.2. Knockdown of RAI3 promotes adipogenic differentiation

To explore the role of *RAI3* on adipogenic differentiation, we established *RAI3* knockdown hASCs. Two different shRNAs (sh*RAI3*-1, sh*RA3*-2) and a non-targeting control shRNA (NC) were introduced into hASCs with lentivirus transfection. Fluorescent staining showed the efficiency of lentiviral transduction was >90% (Fig. 2A). Meanwhile, qRT-PCR and western blot confirmed the expression of *RAI3* was significantly reduced (Fig. 2B–D). After culturing hASCs in adipogenic medium for 21 days, *RAI3* knockdown significantly enhanced adipogenesis as indicated by Oil red O staining (Fig. 2E and F). In agreement with this result, the mRNA levels of the adipogenic specific genes, *PPARγ*, *C/EBPα*, and *ADIPOQ,* were markedly upregulated following the downregulation of *RAI3* (Fig. 2G–I).

3.3. RAI3 knockdown promotes newly generated adipose tissue in vivo

Next, we combined three groups of hASCs (sh*RAI3*-1, sh*RAI3*-2 or NC) with collagen sponge respectively and implanted them into the backs of nude mice to detect the role of *RAI3 in vivo* (Fig. 3A). Both haematoxylin and eosin (H&E) and Oil red O staining showed the *RAI3* knockdown group had more adipose-tissue-like constructs (Fig. 3B).

3.4. RAI3 knockdown inhibits β-catenin accumulation

It is known that Wnt/β-catenin signaling is an important regulator in adipogenesis. We further detected whether *RAI3* regulated adipogenesis through regulating β-catenin expression. Western blot analyses showed that *RAI3* knockdown inhibited the accumulation of β-catenin in total cell lysates (Fig. 4A and B). Given the

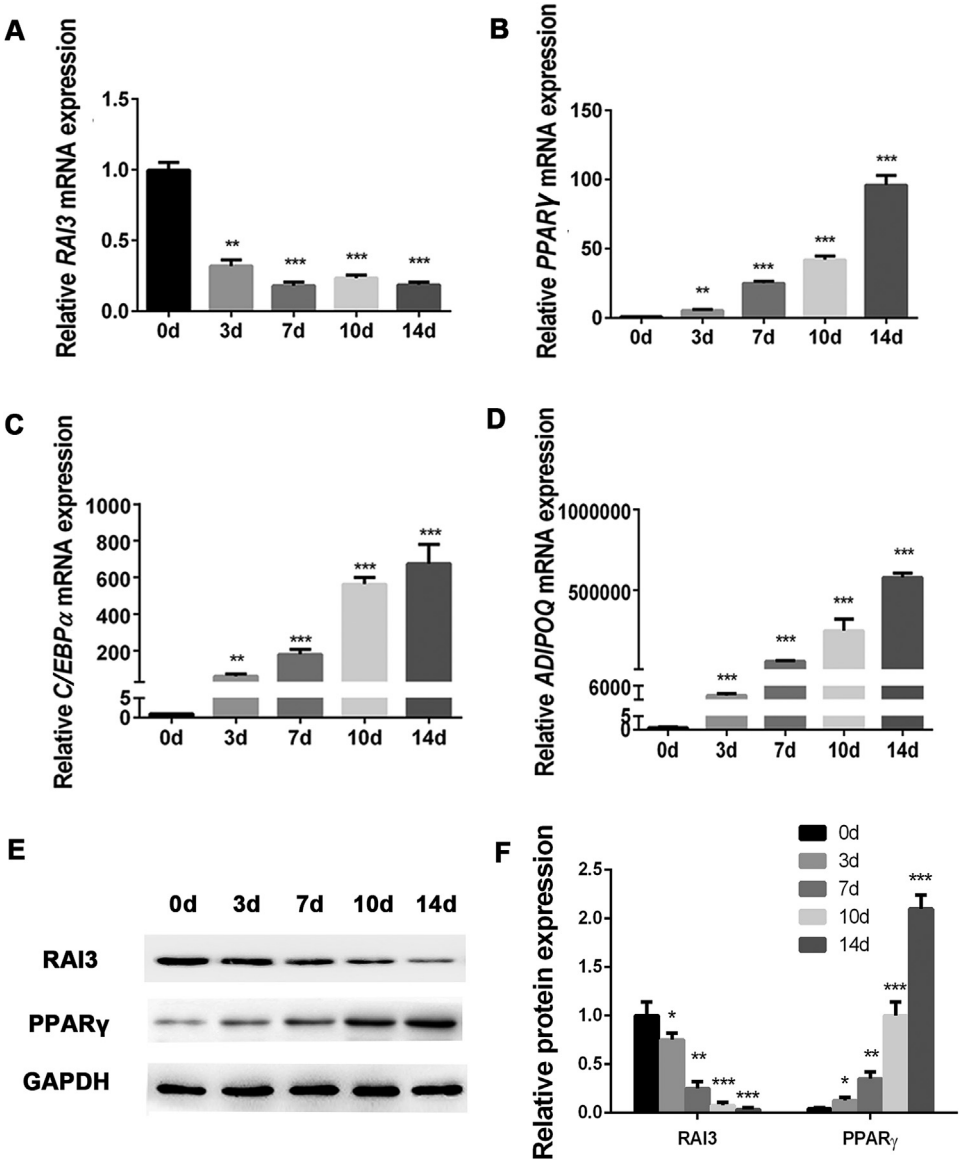

Fig. 1. Downregulation of *RAI3* during the adipogenic differentiation of hASCs. (A) Relative mRNA expression of *RAI3* on day 0, 3, 7, 10 and 14 during adipogenic differentiation of hASCs as determined by qRT-PCR. (B–D) Relative mRNA expression levels of the adipogenic markers *PPARγ* (B), *C/EBPα* (C), and *ADIPOQ* (D) at the indicated time points. (E–F) Western blot analysis (E) and quantification (F) of protein expression of PPARγ, RAI3, and the internal control GAPDH at the indicated time points. All data are presented as mean ± SD (n = 3, $^{*}P < 0.05$, $^{**}P < 0.01$, $^{***}P < 0.001$, compared with day 0).

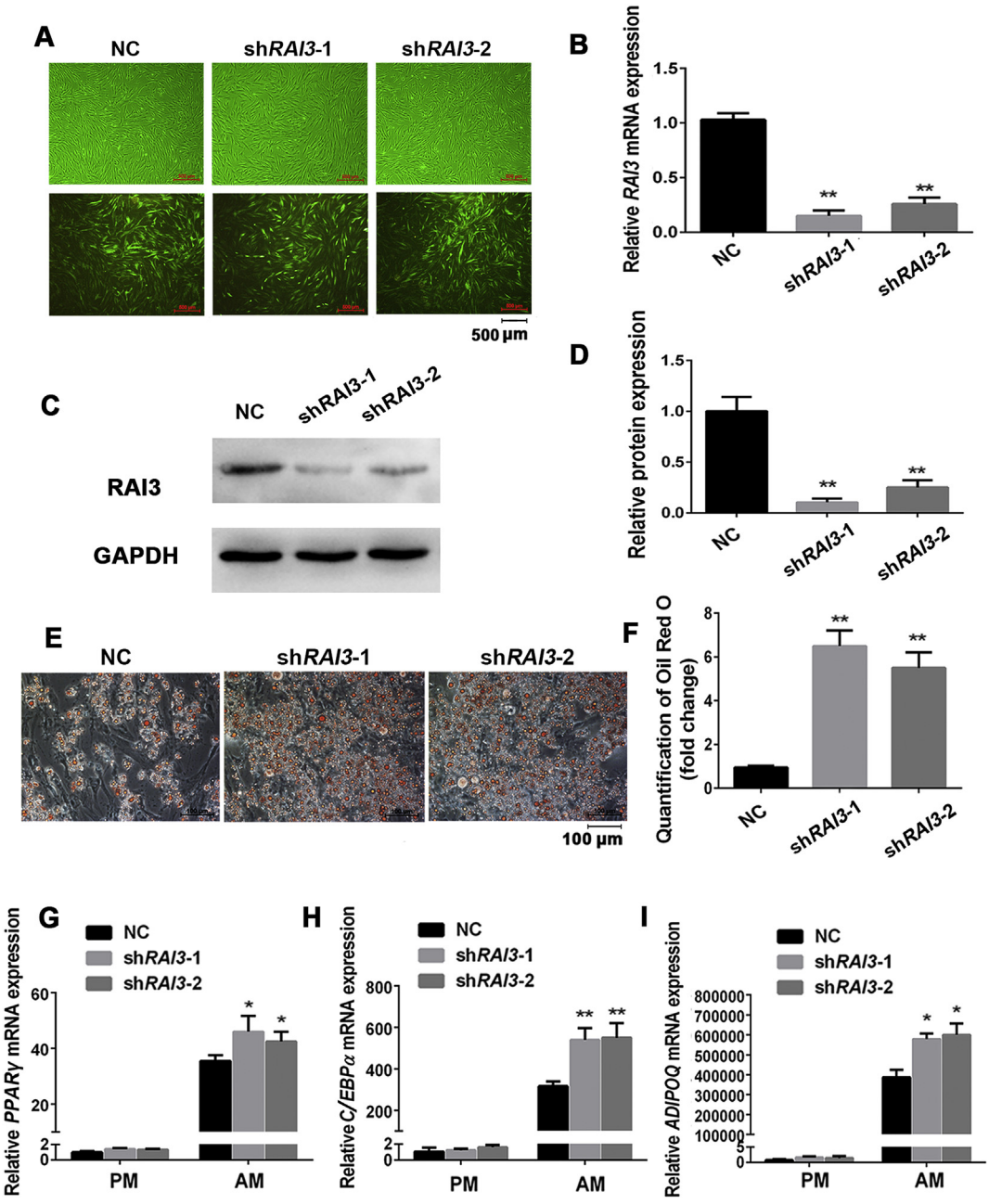

Fig. 2. Knockdown of *RAI3* enhanced adipogenic differentiation of hASCs. The hASCs were transfected with lentivirus expressing sh*RAI3*-1, sh*RAI3*-2, or the non-targeting control shRNA (NC). (A) Fluorescent micrographs show the efficiency of lentivirus transduction (>90%). Scale bar = 500 μm. (B) Histograms show the relative mRNA expression of *RAI3* in the sh*RAI3* groups. (C–D) Knockdown of *RAI3* was also confirmed by western blot analysis (C) and quantification (D). (E–F) Oil red O staining (E) and quantification (F) of cells at day 21 after adipogenic induction. Scale bar = 100 μm. (G–I) Relative mRNA expression of the adipogenic markers *PPARγ*, *C/EBPα*, and *ADIPOQ* assessed by qRT-PCR at day 14 after adipogenic induction. Results are presented as mean ± SD (n = 3, $^{*}P < 0.05$, $^{**}P < 0.01$, compared with NC).

positive role of lithium chloride for Wnt/β-catenin signaling, we treated sh*RAI3*-hASCs with lithium chloride to recover the level of β-catenin (Fig. 4C and D), Oil red O staining showed lithium chloride abolished the promotion of adipogenesis induced by *RAI3* knockdown (Fig. 4E and F).

4. Discussion

Cancer, trauma, and surgery often result in adipose tissue defect which may affect the life quality and mental state of patients [12]. Although traditional strategies for adipose tissue reconstruction such as autologous fat grafting have become common, the outcome of fat grafting is always accompanied by different degrees of volume loss [13]. Recent progress has been made in adipose tissue engineering which provides a new solution for repairing adipose tissue defect. Adipose tissue engineering involves the use of precursor cells, biomaterials and effective factors [14]. Among them, hASCs are considered an ideal cell source for adipose tissue engineering. However, how hASCs differentiate into mature adipocytes remains unclear. Hence it's important to investigate the underlying mechanism of adipogenesis.

Adipogenic differentiation is regulated by a series of

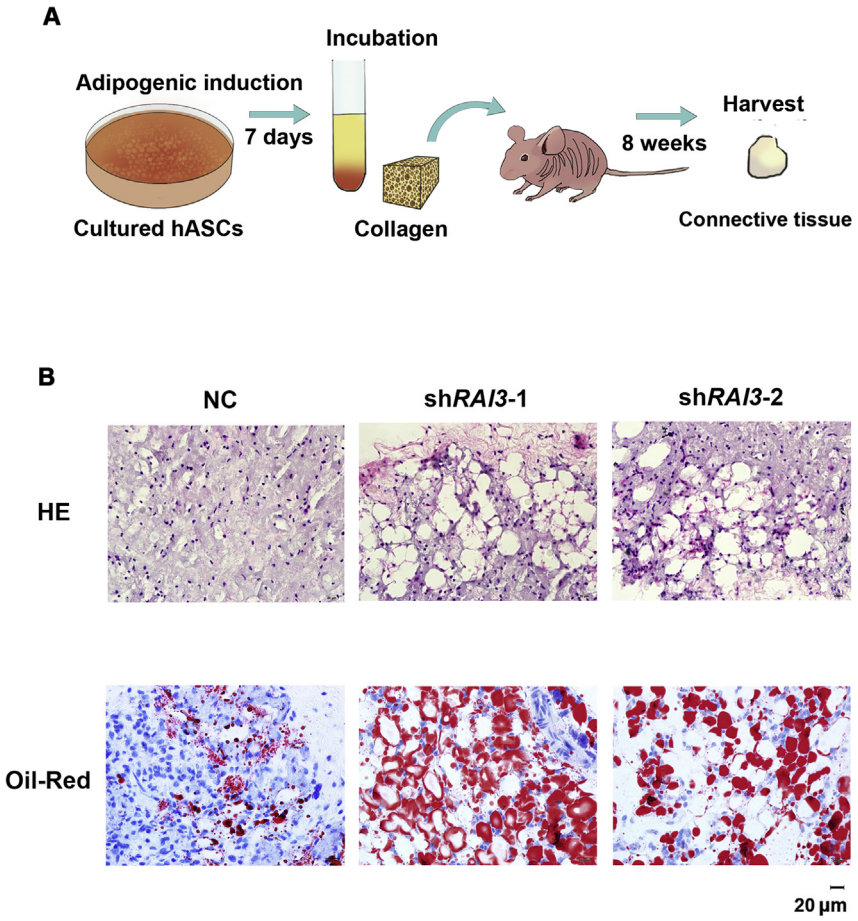

Fig. 3. Knockdown of *RAI3* promoted adipogenesis of hASCs *in vivo*. (A) Schematic diagram illustrating the experimental procedure. (B) H&E staining and Oil red O staining in NC, sh*RAI3*-1, and sh*RAI3*-2 groups. Scale bar = 20 μm.

transcription factors and various pathways. Previous studies have shown that Wnt/β-catenin signaling is one of the central negative regulators of adipogenic differentiation [15]. Wnt signaling is initiated when Wnt glycoprotein ligands bind to frizzled receptors and low density lipoprotein receptor-related protein (LRP) co-receptors, which inhibits glycogen synthase kinase 3β (GSK3β) and then prevents degradation of β-catenin. β-catenin accumulates and translocates into the nucleus where it binds to T-cell factor/lymphoid-enhancer factor family of transcription factors, resulting in inhibition of adipogenic transcription factors PPARγ and C/EBPα [16–18]. As is well known, LiCl is an agonist of Wnt/β-catenin signaling through repressing the activity of GSK3β and stabilizing β-catenin [19].

RAI3, also known as G-protein–coupled receptor family C group 5 type A (*GPRC5A*) or retinoic acid-inducible gene 1 (*RAIG1*), is a member of the largest and most abundant receptor family in mammals [20]. *RAI3* is located on chromosome 12p13-p12.3 and initially reported to be strongly expressed in the lung [21,22]. Since then, *RAI3* has been found to play significant roles in several biological processes, such as tumorigenesis, cell proliferation, inflammation, and cell cycle progression [23–25]. But research into the function of *RAI3* in adipogenesis is lacking.

In this study, we found that *RAI3* expression was significantly downregulated during adipogenesis of hASCs. Thus, we speculated that *RAI3* was a negative regulator of adipogenic differentiation. We generated *RAI3* knockdown hASCs by lentivirus transfection. In vitro studies showed that *RAI3* knockdown cells had more lipid accumulation and higher expression of adipogenic marker genes compared with control groups. In addition, we found *RAI3* silence significantly decreased the level of β-catenin. Since previous studies have demonstrated that downregulation of β-catenin is coincident with the increase of PPARγ in mesenchymal stem cells [26], we hypothesized that *RAI3* knockdown promoted adipogenesis through decreasing the level of β-catenin. To prove the hypothesis, cells were pretreated with LiCl to upregulate β-catenin accumulation. The results displayed that LiCl abolished the positive effect of *RAI3* knockdown on adipogenesis. Thus, *RAI3* knockdown promotes adipogenesis at least partially through suppression of β-catenin expression. Taken together, the present study discovered the significant role of *RAI3* on the adipogenesis.

Although we found *RAI3* knockdown promoted adipogenesis through impacting β-catenin expression, besides β-catenin, many other transcription factors also regulate adipogenesis, such as PPARγ, C/EBPα [27]. Zhou et al. found cathepsin B promoted pre-adipocyte differentiation by degrading fibronectin and inhibiting Wnt/β-catenin signaling [28]. H. Okamura et al. found serine/threonine protein phosphatase 2A (PP2A) regulated adipogenesis by regulating the Wnt/GSK-3β/β-catenin pathway and PPARγ expression [29]. Hence, *RAI3* may regulate adipogenesis by other mechanisms, such as interacting with PPARγ.

Adipose tissue engineering provides a novel solution for restoring adipose tissue defect result from cancer, congenital malformation, or injury. In this study, our results showed that *RAI3* knockdown promoted newly generated adipose tissue *in vivo*,

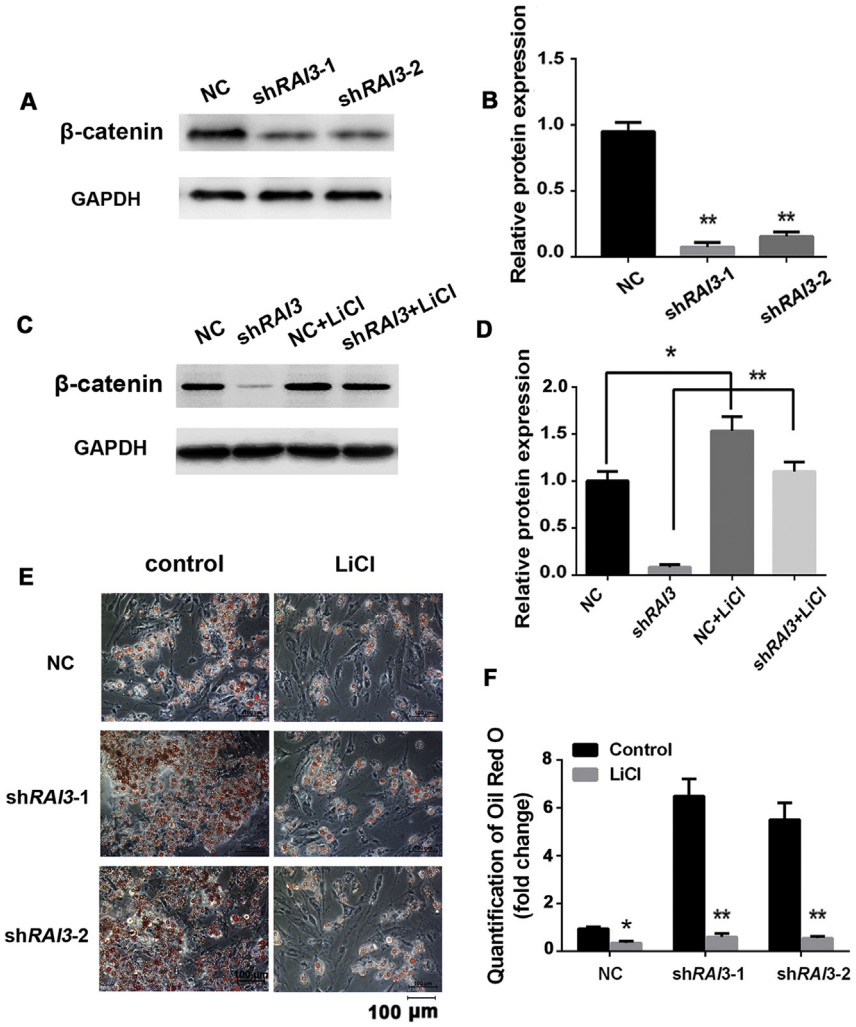

Fig. 4. *RAI3* knockdown reduced the level of β-Catenin. (A–B) Western blot analysis (A) and quantification (B) showed *RAI3* knockdown downregulated the protein level of β-catenin (compared with NC). (C–D) Expression of β-catenin was examined by western blot (C) in the presence of lithium chloride (LiCl) (5 mmol/L). Histograms show the quantification (D) of band intensities. (E–F) Oil red O staining (E) and quantification (F) of cells at day 21 after adipogenic induction (normalized to control groups). Results are presented as mean ± SD (n = 3, $^{*}P < 0.05$, $^{**}P < 0.01$).

which indicated the potential use of *RAI3* as a molecular target for adipose tissue regeneration.

In summary, this study discovered the facilitating effect of *RAI3* knockdown on the adipogenesis of hASCs. Furthermore, we have demonstrated that *RAI3* knockdown stimulated adipogenesis was coincident with the decrease of β-catenin. However, the underlying mechanisms are not completely understood, further research is needed to clarify the effect of *RAI3* on adipogenesis.

Acknowledgements

C.J. conceived the experiments, performed the experiments, collecting the data, analyzed the data, prepared the figures, and wrote the main manuscript text. W.W. performed experiments, collecting the data. Y.L. and Y.Z. conceived the experiments, supervised the work, and edited the manuscript. All authors approved the final version of the manuscript.

Funding

This study was supported by grants from the National Natural Science Foundation of China (81570953 and 81500822) and the Project for Culturing Leading Talents in Scientific and Technological Innovation of Beijing (Z171100001117169).

Competing financial interests

The authors declare no competing financial interests.

Transparency document

Transparency document related to this article can be found online at http://dx.doi.org/10.1016/j.bbrc.2017.08.142.

References

[1] M. Esteve Rafols, Adipose tissue: cell heterogeneity and functional diversity, Endocrinol. Nutr. 61 (2014) 100–112.
[2] D.A. Young, Y.S. Choi, A.J. Engler, K.L. Christman, K.L. Christman, Stimulation of adipogenesis of adult adipose-derived stem cells using substrates that mimic the stiffness of adipose tissue, Biomaterials 34 (2013) 8581–8588.
[3] S.R. Farmer, Transcriptional control of adipocyte formation, Cell Metab. 4 (2006) 263–273.
[4] Y. Sakaguchi, I. Sekiya, K. Yagishita, T. Muneta, Comparison of human stem cells derived from various mesenchymal tissues: superiority of synovium as a cell source, Arthritis Rheumatol. 52 (2005) 2521–2529.
[5] A. Zougman, G.G. Hutchins, D.A. Cairns, E. Verghese, S.L. Perry, D.G. Jayne,

P.J. Selby, R.E. Banks, Retinoic acid-induced protein 3: identification and characterisation of a novel prognostic colon cancer biomarker, Eur. J. Cancer 49 (2013) 531–539.
[6] L. Cheng, S. Yang, Y. Yang, W. Zhang, H. Xiao, H. Gao, X. Deng, Q. Zhang, Global gene expression and functional network analysis of gastric cancer identify extended pathway maps and GPRC5A as a potential biomarker, Cancer Lett. 326 (2012) 105–113.
[7] A.P. Sokolenko, D.R. Bulanova, A.G. Iyevleva, S.N. Aleksakhina, E.V. Preobrazhenskaya, A.O. Ivantsov, E.S. Kuligina, N.V. Mitiushkina, E.N. Suspitsin, G.A. Yanus, O.A. Zaitseva, O.S. Yatsuk, A.V. Togo, P. Kota, J.M. Dixon, A.A. Larionov, S.G. Kuznetsov, E.N. Imyanitov, High prevalence of GPRC5A germline mutations in BRCA1-mutant breast cancer patients, Int. J. Cancer 134 (2014) 2352–2358.
[8] J. Fujimoto, H. Kadara, M.M. Garcia, M. Kabbout, C. Behrens, D.D. Liu, J.J. Lee, L.M. Solis, E.S. Kim, N. Kalhor, C. Moran, A. Sharafkhaneh, R. Lotan, I.I. Wistuba, G-protein coupled receptor family C, group 5, member A (GPRC5A) expression is decreased in the adjacent field and normal bronchial epithelia of patients with chronic obstructive pulmonary disease and non-small-cell lung cancer, J. Thorac. Oncol. 7 (2012) 1747–1754.
[9] W.P. Cawthorn, A.J. Bree, Y. Yao, B. Du, N. Hemati, G. Martinez-Santibanez, O.A. MacDougald, O.A. MacDougald, Wnt6, Wnt10a and Wnt10b inhibit adipogenesis and stimulate osteoblastogenesis through a beta-catenin-dependent mechanism, Bone 50 (2012) 477–489.
[10] K.L. Lauing, S. Sundaramurthy, R.K. Nauer, J.J. Callaci, Exogenous activation of Wnt/beta-catenin signaling attenuates binge alcohol-induced deficient bone fracture healing, Alcohol Alcoholi 49 (2013) 399–408.
[11] P. Zhang, Y. Liu, C. Jin, M. Zhang, F. Tang, Y. Zhou, Histone acetyltransferase GCN5 regulates osteogenic differentiation of mesenchymal stem cells by inhibiting NF-kappaB, J. Bone Min. Res. 31 (2016) 391–402.
[12] Z. Peng, Z. Dong, Q. Chang, W. Zhan, Z. Zeng, S. Zhang, F. Lu, Tissue engineering chamber promotes adipose tissue regeneration in adipose tissue engineering models through induced aseptic inflammation, Tissue Eng. Part C 20 (2014) 875–885.
[13] W. Zhu, C.M. Nelson, Adipose and mammary epithelial tissue engineering, Biomatter 3 (2013).
[14] L. Wang, Q. Johnson Ja Fau - Zhang, E.K. Zhang Q Fau - Beahm, E.K. Beahm, Combining decellularized human adipose tissue extracellular matrix and adipose-derived stem cells for adipose tissue engineering, Acta Biomater. 9 (2013) 8921–8931.
[15] X. Chen, Y. Luo, G. Jia, G. Liu, H. Zhao, Z. Huang, FTO promotes adipogenesis through inhibition of the Wnt/beta-catenin signaling pathway in porcine intramuscular preadipocytes, Anim. Biotechnol. (2017) 1–7.
[16] S. Kang, C.N. Bennett, I. Gerin, L.A. Rapp, K.D. Hankenson, O.A. Macdougald, Wnt signaling stimulates osteoblastogenesis of mesenchymal precursors by suppressing CCAAT/enhancer-binding protein alpha and peroxisome proliferator-activated receptor gamma, J. Biol. Chem. 282 (2007) 14515–14524.
[17] T.C. Prestwich, O.A. Macdougald, Wnt/beta-catenin signaling in adipogenesis and metabolism, Curr. Opin. Cell Biol. 19 (2007) 612–617.
[18] J.A. Kennell, O.A. MacDougald, Wnt signaling inhibits adipogenesis through beta-catenin-dependent and independent mechanisms, J. Biol. Chem. 280 (2005) 24004–24010.
[19] C.M. Hedgepeth, J. Conrad Lj Fau - Zhang, H.C. Zhang J Fau - Huang, V.M. Huang Hc Fau - Lee, P.S. Lee Vm Fau - Klein, P.S. Klein, Activation of the Wnt signaling pathway: a molecular mechanism for lithium action, Dev. Biol. 185 (1997) 82–91.
[20] H. Jorissen, N. Bektas, E. Dahl, A. Hartmann, A. ten Haaf, S. Di Fiore, H. Kiefer, A. Thess, S. Barth, T. Klockenbring, Production and characterisation of monoclonal antibodies against RAI3 and its expression in human breast cancer, BMC Cancer 9 (2009) 200.
[21] Y. Cheng, R. Lotan, Molecular cloning and characterization of a novel retinoic acid-inducible gene that encodes a putative G protein-coupled receptor, J. Biol. Chem. 273 (1998) 35008–35015.
[22] Q. Tao, J. Fujimoto, T. Men, X. Ye, J. Deng, L. Lacroix, J.L. Clifford, L. Mao, C.S. Van Pelt, J.J. Lee, D. Lotan, R. Lotan, Identification of the retinoic acid-inducible Gprc5a as a new lung tumor suppressor gene, J. Natl. Cancer I 99 (2007) 1668–1682.
[23] X. Lin, S. Zhong, X. Ye, Y. Liao, F. Yao, X. Yang, B. Sun, J. Zhang, Q. Li, Y. Gao, Y. Wang, J. Liu, B. Han, Y.E. Chin, B.P. Zhou, J. Deng, EGFR phosphorylates and inhibits lung tumor suppressor GPRC5A in lung cancer, Mol. Cancer 13 (2014) 233.
[24] M. Hirano, L. Zang, T. Oka, Y. Ito, Y. Shimada, Y. Nishimura, T. Tanaka, Novel reciprocal regulation of cAMP signaling and apoptosis by orphan G-protein-coupled receptor GPRC5A gene expression, Biochem. Bioph. Res. Co. 351 (2006) 185–191.
[25] H. Zhou, I. Rigoutsos, The emerging roles of GPRC5A in diseases, Oncoscience 1 (2014) 765–775.
[26] S. Rahman, P.J. Czernik, Y. Lu, B. Lecka-Czernik, Beta-catenin directly sequesters adipocytic and insulin sensitizing activities but not osteoblastic activity of PPARgamma2 in marrow mesenchymal stem cells, Plos One 7 (2012) e51746.
[27] A.W. James, Review of signaling pathways governing MSC osteogenic and adipogenic differentiation, Scientifica 2013 (2013) 684736.
[28] Z.Y. Zhang, Y. Mai, H. Yang, P.Y. Dong, X.L. Zheng, G.S. Yang, CTSB promotes porcine preadipocytes differentiation by degrading fibronectin and attenuating the Wnt/beta-catenin signaling pathway, Mol. Cell. Biochem. 395 (2014) 53–64.
[29] H. Okamura, D. Yang, K. Yoshida, J. Teramachi, T. Haneji, Reduction of PP2A Calpha stimulates adipogenesis by regulating the Wnt/GSK-3beta/beta-catenin pathway and PPARgamma expression, BBA-Mol. Cell Res. 1843 (2014) 2376–2384.